A Stretchable Glucose Sensor via Conductive Polymer-coated VACNT Forests Rooted in Elastomer Polymer Substrate

Anthony Palumbo, *Member, IEEE*, Hongjun Wang, Kalle Levon, and Eui-Hyeok Yang, *Senior Member*, *IEEE*

***Abstract*—This paper presents a stretchable glucose sensor composed of dodecylbenzenesulfonate-doped polypyrrole (PPyDBS)-coated vertically aligned carbon nanotube (VACNT) forests rooted in polydimethylsiloxane (PDMS) substrate. The measured sensitivity was approximately 10 mA cm^{-2} M^{-1} with a wide linear range demonstrated, as low as 0.1 mM and up to 12 mM, and the sensor achieved 90% of steady-state current in less than 3 seconds. The PDMS/CNT/PPy(DBS)/GOx structure was tested under stretching, demonstrating the coefficients of determination larger than 0.982, indicating its robustness of sensing capability of glucose concentrations with tensile strain up to 75%. These results show the potential of this stretchable glucose sensor with a novel fabrication strategy and stretchable electrode design toward potential wearable applications interfacing with physiological fluids.**

***Index Terms*—** Carbon nanotubes, stretchable electrode, electrochemical sensing, glucose sensor, conjugated polymer

Manuscript received March X, 2022; accepted XXX. Date of publication XXX; date of current version XXX. The authors acknowledge partial support by the Air Force Office of Scientific Research under Grant FA9550-11-10272. This research used microscopy resources, partially funded by the NSF via Grant NSF-DMR-0922522, within the Laboratory for Multiscale Imaging (LMSI) at Stevens Institute of Technology. This work was also partially carried out at the Micro Device Laboratory (MDL) at Stevens Institute of Technology, funded with support from W15QKN-05-D-0011.

Anthony Palumbo is with the Mechanical Engineering Department, Stevens Institute of Technology, Hoboken, NJ, United States. (e-mail: aplumbo@stevens.edu)

Hongjun Wang is with the Biomedical Engineering Department, Stevens Institute of Technology, Hoboken, NJ, United States. (e-mail: hwang2@stevens.edu)

Kalle Levon is with the Chemical and Biomolecular Engineering, Tandon School of Engineering, Six Metrotech Center, Brooklyn, NY, United States. (e-mail: klevon@nyu.edu)

Eui-Hyeok Yang is with the Mechanical Engineering Department, Stevens Institute of Technology, Hoboken, NJ 07030, USA, and with Center for Quantum Science and Engineering, Stevens Institute of Technology, Hoboken, NJ, United States, as well as the Center for Quantum Science and Engineering, Stevens Institute of Technology, Hoboken, NJ, United States. (e-mail: eyang@stevens.edu)

I. INTRODUCTION

THE incorporation of sensing materials with flexible and stretchy materials enables electronic skins [1], smart sensor bandages [2], and wearable medical devices [3]. Human activity often induces multiscale and dynamic deformations, such as at the site of joints, which often accommodate more than 50% stretchability deformation [4]. Stretchable biosensors are used to detect stimuli of the human body, which are often not flat and constantly moving [5]–[8], and these sensors benefit from uninterrupted attachment to the surface environment to provide continuous measurements. In addition to site monitoring, stretchable sensors can monitor the entire human system, such as in medical diagnostics for continuous monitoring [9]. Among the various wearable biosensors, electrochemical sensors are a developing field for monitoring vital signals via detecting physiological components in human fluids with the advantages of non-invasive and high-specificity sensing [10], [11]. While invasive glucose sensors are mainstream for determining glucose levels in the blood, non-invasive glucose sensors have been shown with external physiological fluids, such as sweat [9] and ocular fluid [10], minimizing pain and infections caused by an invasive nature [11, 12]. Physiological fluids contain metabolites and electrolytes, which provide valuable information about a patient's health and condition [12]. Therefore, stretchable sensors capable of measuring fluids enable disease diagnosis in a real-time and comfortable manner.

Wearable or skin-attachable electrodes can be subjected to various lateral strains and accommodate significant bending, twisting, and stretching [11]. The stretchable electrodes are often synthesized with elastomeric polymer substrates, including polyimide, polydimethylsiloxane (PDMS), poly (methyl methacrylate) (PMMA), and polyethylene (PE) [13, 14]. Typically, a sensor requires a transducer element to convert a stimulus into a recordable electronic signal, often through functionalized conductive electrodes. To achieve conductive transducer functionality, flexible substrates are conventionally deposited with thin metal films, including Au, Ag, and Pt [15-17]. However, mechanical deformation can lead to crack propagation and/or delamination of the films from the underlying stretchable substrate, causing inconsistent readings and premature device failure [18, 19]. One can combine conductive materials that can undergo strain on par with the capability of their underlying flexible substrates. For example, conductive networks can be formed using carbon nanotubes (CNTs) as observed by forests of vertically aligned CNTs (VACNTs) [20, 21], which are often combined with either polyethylene terephthalate (PET) or polycarbonate (PC) [22-24]. In addition, CNT-based stretchable electrodes on elastomeric substrates have demonstrated high flexibility, limited only by the cohesive fracture of elastomeric substrates [25, 26]. CNTs can also be combined with conjugated polymers for biosensing applications as the sensing or supporting matrix, whereby CNTs imbue mechanical support to maintain the structural integrity of the matrix [27-29]. Polypyrrole (PPy) is a popular conjugated polymer for flexible and stretchable electrodes [35], which is typically doped with cations to achieve

This article has been accepted for publication in IEEE Journal on Flexible Electronics. This is the author's version which has not been fully edited and content may change prior to final publication. Citation information: DOI 10.1109/JFLEX.2023.3288501

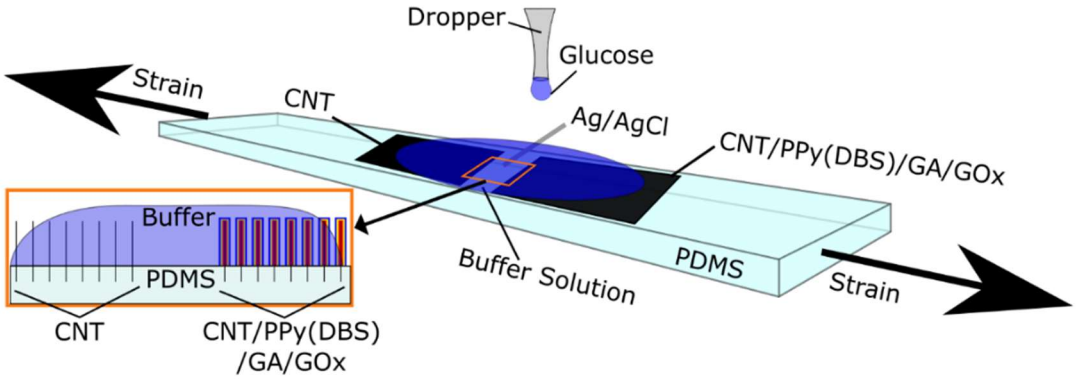

Figure 1. Illustration of the stretchable glucose sensor.

higher conductivity [30-32]. PPy can also immobilize various enzymes in electrochemical sensor designs, most notably glucose oxidase (GOx), towards glucose detection [33-36].

To date, efforts have been pursued to incorporate PPy with CNTs in developing glucose sensors with GOx, as shown in Table S1. Further information on enzyme-based sensors and the sensing mechanism is included herewith. Furthermore, various strategies have been reported to obtain flexible glucose sensors with other materials, as shown in Table S2. Several strategies have been pursued to detect glucose levels in various physiological fluids that enable non-invasive operation, such as optical and microwave sensors [37-39]; however, those with flexibility are more limited [40-52]. While various CNT/PPy composites have been used as electrode materials in GOx-based glucose sensing [53-59], none of the previous reports demonstrated stretchable glucose sensing. Incorporating these materials into stretchable electrodes would be beneficial to realizing wearable glucose sensors for continuous monitoring.

Here, we demonstrate a stretchable glucose sensor platform to detect glucose by up to 75% of strain applications. The chemical vapor deposition (CVD)-grown VACNTs rooted in PDMS allow for a stretchable electrode design [60-63], which are comprehensively tested for GOx-based glucose detection under stretching. We show that a conformal coating of PPy(DBS) thin film on individual VACNTs via electropolymerization maintains the structure's integrity under a tensile strain up to at least 75%. GOx immobilized on the PPy(DBS) surface allows selective sensing of glucose. The resulting PDMS/VACNTs/PPy(DBS)/GOx is exposed to iterative glucose concentrations, resulting in a concentration-dependent change of measurable current. We demonstrate that conformal coating of PPy(DBS) onto individual CNT surfaces facilitates increased reaction sites, resulting in at least 4 times higher sensitivity than observed with independent PPy(DBS) films. Furthermore, we demonstrate that the sensor produces a proportional response to changes in glucose concentration, with tensile strains of 0%, 15%, 30%, 45%, 60%, and 75%.

II. MATERIALS AND METHODS

A. Preparation of PDMS/CNT/PPy(DBS) Electrodes and GOx Immobilization

The PDMS/CNT electrode template and its fabrication has been reported elsewhere [60-63]. A detailed description of the preparation of PDMS/CNT/PPy(DBS) electrodes is found in the SUPPLEMENTARY MATERIAL. VACNT forests were grown via APCVD and characterized using Raman spectroscopy to confirm the integrity of individual nanotubes despite the later strain of the substrate, as shown in Figure S1 and our previous work [60-63]. Further details regarding the characterization methods are included herewith. Figure S2 shows the Raman spectroscopy of the Si/SiO_2 substrate with CNT (before transfer onto PDMS) and without CNT (after transfer).

GOx was immobilized onto the working electrode using glutaraldehyde (GA) as a crosslinking agent. The PDMS/CNT/PPy(DBS) was first dipped in 0.25 wt% GA solution, left for 1.5 hours at room temperature and washed 2-3 times with 0.1 M potassium phosphate buffer. Next, the stock solution of GOx (2 mg/mL) prepared in 0.1 M potassium phosphate buffer (pH 7) was used to adsorb GOx onto the PPy(DBS) surface. Next, PDMS/CNT/PPy(DBS) was dipped into the GOx solution for 2 hours at 4 °C, followed by washing 2-3 times with 0.1 M potassium phosphate buffer. The incorporation of GA media resulted in an immobilization with better physical and chemical stability of the catalytic material due to crosslinking formed with GA and GOx [56, 64-66]. By doing so, active sites of GOx can be more accessible for enzymatic activity. These methods were also employed to immobilize GOx on CNT and PPy(DBS) electrodes used for comparison. Figure S3 shows the schematic diagram for the preparation process for the working electrode of the glucose sensor.

B. Characterization of Glucose Concentrations

For experiments comparing CNT, PPy(DBS), and CNT/PPy(DBS), the following were used as samples: (1) as-grown CNT transferred onto PDMS, (2) electropolymerized PPy(DBS) film coating on a flat Au-coated Si/SiO_2 chip, and (3) CNT coated with PPy(DBS) on a PDMS substrate, with fabrications as described in the above sections; GOx was

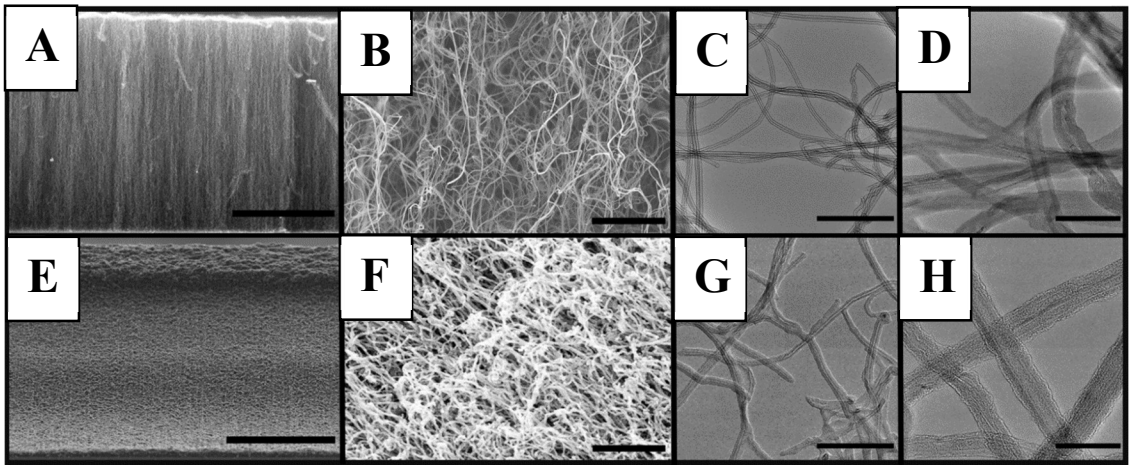

Figure 2. SEM images of (A) side view of bare vertically aligned CNTs and (E) side view of PPy(DBS)-coated CNTs of approximately 100 µm height with a scale bar of 50 µm; SEM images of (B) side view of bare CNTs and (F) top view of PPy(DBS)-coated CNTs with a scale bar of 750 nm; TEM images of (C) bare CNTs and (G) PPy(DBS)-coated CNTs with a scale bar of 250 nm; TEM images of (D) bare CNTs and (H) PPy(DBS)-coated CNTs with a scale bar of 50 nm.

immobilized on each of these samples following the same procedure described above as well. The experimental setup is shown in Figure S4 with further details. The samples acted as working electrodes and were inserted into a solution of 20 mL of 0.1 M phosphate buffer (pH 7) with a CNT counter electrode and an Ag/AgCl reference electrode. A constant voltage of 0.65 V was applied, and glucose concentration-dependent current changes were observed upon successive additions of 0.2 mM glucose (i.e., 4 µL of 1 M glucose) up to 0.8 mM, followed by successive additions of 0.4 mM glucose (i.e., 8 µL of 1 M glucose) up to 4.8 mM, and followed by 0.8 mM glucose (i.e., 16 µL of 1 M glucose) up to 12.8 mM at intervals of 50 s. Selection of the 0.65 V constant electrochemical potential was determined using data obtained via cyclic voltammetry as outlined in the Results and Discussion section and Figure S5. For interference testing, the same setup was pursued with a CNT/PPy(DBS)/GOx working electrode and an injection of 1.5 mM glucose into the phosphate buffer solution, followed by successive additions of 0.1 mM ascorbic acid (AA), 10 mM urea, 150 mM sodium chloride (NaCl), and 0.1 mM uric acid (UA) with 50 s intervals at a constant potential of 0.65 V. For glucose testing performed with application of tensile strain, as shown in Figure 1, a single PDMS substrate containing CNT as counter electrode and CNT/PPy(DBS)/GOx as working electrode spaced apart several mm was used for testing with an Ag/AgCl wire reference electrode. 2 mL of buffer solution was placed centrally on the sensor. Successive additions of 0.8 mM glucose were added to the solution to observe glucose concentration-dependent current changes. The tensile strain was applied with a clamped system with 15%, 30%, 45%, 60%, and 75% strains. As commonly employed in tensile strain experiments, one side clamp held the sample, while the other clamp moved laterally to stretch the sample [67-69].

III. RESULTS AND DISCUSSION

A. Glucose Sensor

Figure 2 shows SEM and TEM images of CNTs with and without PPy(DBS) coatings. We previously showed that incorporating DBS^- molecules assists in a conformal coating of PPy to provide easy access of ions to individual coated CNTs [63]. Additional images and details regarding the polymer coating process of PPy(DBS)-coated CNTs are shown in Figure S6. A detailed description of PPy(DBS) coating process is published elsewhere [70-76], and described in detail in SUPPLEMENTARY MATERIAL.

The electropolymerized PPy(DBS) film conformally coats individual CNTs, corresponding to an average CNT diameter of approximately 10 nm with an average PPy(DBS) conformal film thickness of approximately 9 nm. In addition, the existing spacing between CNTs allows for the diffusion of glucose within the surrounding liquid medium. In this way, more glucose molecules would access potential reaction sites where a reaction occurs in the presence of glucose oxidase, resulting in a change in current. While the dip-coating procedures of GA and GOx functionalize the electrode towards sensing glucose, its presence was confirmed by observing the working electrode's electrochemical performance in the presence of glucose. The protein molecules, GOx, are not easily visible in conventional imaging procedures. These biological samples would require complex preparations and specific staining procedures to enhance contrast adequately to be observable by electron microscope methods [77, 78].

B. Glucose Sensing without Strain

Figure 3a shows a typical response current vs. time plot for the biosensor at 0.65 V (vs. Ag/AgCl) applied between a CNT counter electrode and the fabricated PDMS/CNT/PPy(DBS)/GOx working electrode shown in Figure S3. The electrochemical behavior of the PDMS/CNT/PPy(DBS)/GOx electrode under glucose additions was investigated by chronoamperometry. Iterative glucose concentrations were added to the buffer solution, and GOx

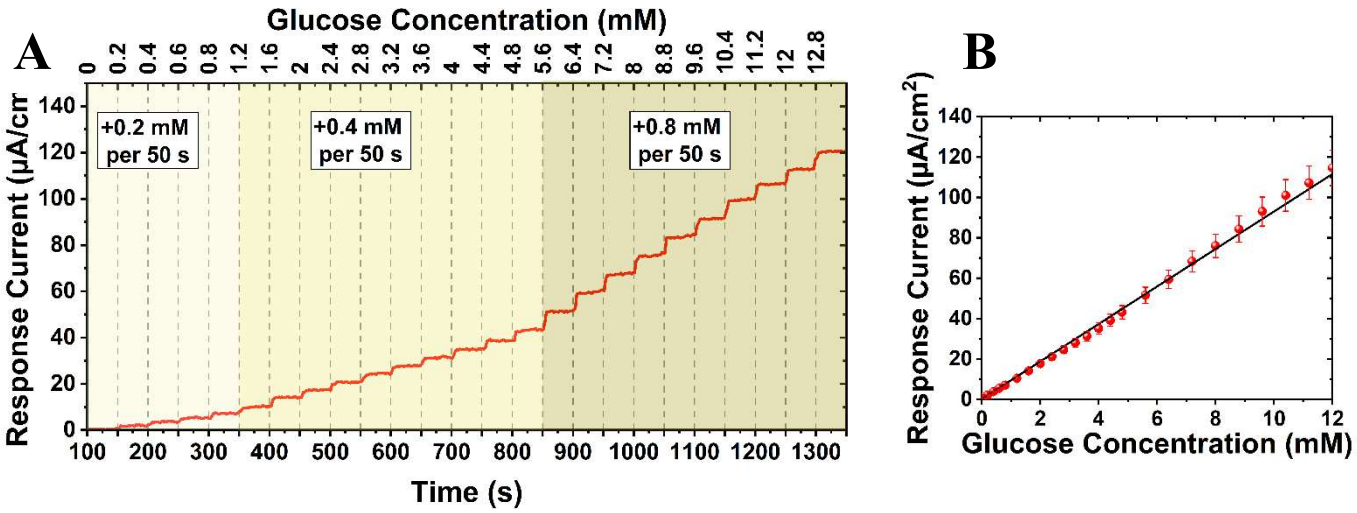

Figure 3. (A) Current response of PDMS/CNT/PPy(DBS)/GOx upon successive addition of glucose at 50-second intervals, and (B) linear regression of the mean current response and standard deviation, averaged with four differing datasets.

reacted in the presence of glucose, resulting in a concentration-dependent change of measurable current. When a measurable amount of glucose solution was added, the oxidation current exhibited a stepwise behavior, reaching a higher state nearly instantly. The sensor achieved 90% of steady-state current in less than 3 seconds. A response time of < 3 seconds would enable the use of this system for continuous monitoring systems [79, 80]. Three different regions are illustrated in the graph corresponding to additions at 50 s intervals of 0.2 mM, 0.4 mM, and 0.8 mM intervals, respectively. A sensitivity of approximately 10 mA cm^{-2} M^{-1} and a wide range were observed with glucose concentrations as low as 0.1 mM and up to 12 mM with a highly linear response trend. A strong correlation of the average current response of four different sensors with a coefficient of determination of 0.998 is shown in Figure 3b, a consistent amount for the different regions of increasing additions of glucose concentration.

Figure 4a shows the response current vs. time for three different types of electrodes: (1) CNT/PPy(DBS), (2) CNT, and (3) PPy(DBS). Figure S7 shows the same graphs with the logarithmic scale in the y-axis to show the very low values/curves. GOx was deposited using the same method onto each substrate via dip-coating with 0.25 wt% GOx solution. GA was used for each deposition of GOx as a crosslinker agent to encourage adhesion to the surfaces and chemical reaction kinetics. The electrodes were supplied with constant voltages of 0.65 V for 100 s to achieve a steady-state before adding glucose solution. Successive aliquots of glucose were added to the buffer solution at 50 s intervals to achieve successive concentrations of 0.4 mM of glucose. The voltage of 0.65 V was chosen as shown in previous works involving PPy(DBS) combined with GOx [81-83]. Hydrogen peroxide production was accomplished as shown by high values of anodic current achieved at this voltage, which agrees with the reaction mechanism proposed for glucose oxidation in the presence of GOx [84, 85]. To confirm the use of this voltage with the PDMS/CNT/PPY(DBS)/GOx electrode, cyclic voltammetry was performed. As shown in Figure S4, when the sensor was in

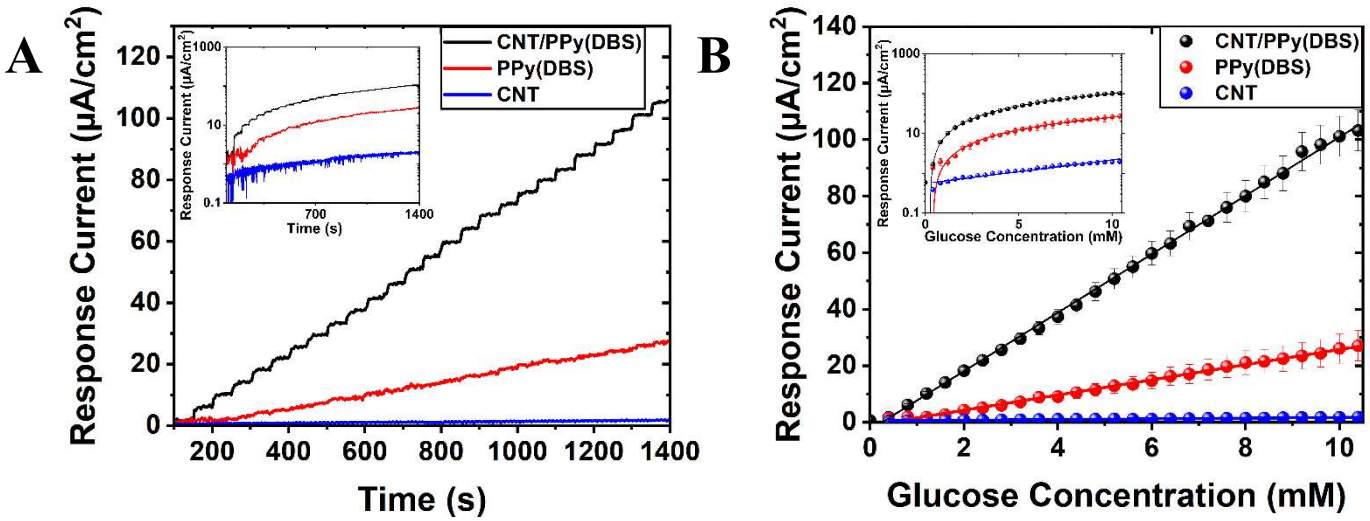

Figure 4. (A) Current response of PPy(DBS)-coated CNTs, PPy(DBS), and CNTs upon successive addition of glucose, and (B) the linear calibration curves for CNT/PPy(DBS), PPy(DBS) and CNT between the response current and the glucose concentration. An insert of logarithmic scale can be seen in each plot.

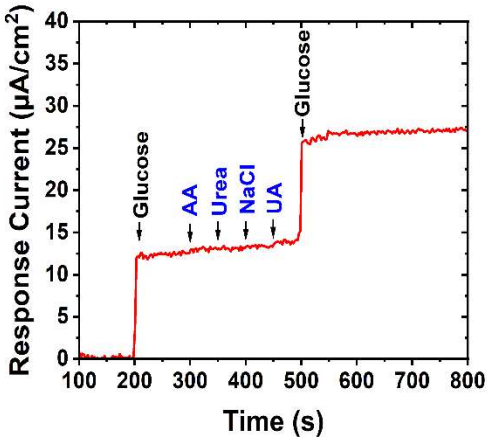

Figure 5. Response current of PDMS/CNT/PPy(DBS)/GOx electrode after addition of 1.5 mM glucose followed by successive addition of 0.1 mM AA, 10 mM urea, 150 mM NaCl, and 0.1 mM UA with 50 s intervals into stirring solution at a constant potential of 0.65 V.

the presence of glucose, H2O2 was generated and led to an anodic current at the electrode, polarized at 0.65 V. This further justifies the use of 0.65 V in these experiments. The combination of CNT/PPy(DBS) demonstrated the advantages of using these materials together in the unique combination reported herein rather than individually. Compared to the PPy(DBS) thin-film on a flat Au-coated Si/SiO_2 chip, the PPy(DBS) conformally-coated on VACNT has a larger effective surface area than the flat PPy(DBS). Therefore, the fast response time in this sensor implies the effectiveness of increased surface area of the CNT/PPy(DBS) electrode due to the conformal coating of PPy(DBS) on individual CNTs.

As shown in Figure 4, PPy(DBS) coated on CNTs resulted in at least 400% improved sensitivity and at least approximately 0.2% increase in the linear coefficient of determination than either material independently with a linear calibration curve between the current and the glucose concentration. CNT forests offer high conductivity, commonly ranging from 7 to 14 S cm^{-1} along with the array at 300 K [86], in addition to geometric favorability of high specific surface area. Conformal coating of PPy(DBS) onto individual CNT surfaces increased reaction sites, resulting in approximately 4 times higher sensitivity than observed with independent PPy(DBS) films. Figure 4b shows the calibration curve of the PPy(DBS). The coefficients of determination for PPy(DBS)/CNT, PPy(DBS), and CNT, were 0.998, 0.997, and 0.976, respectively. The calibration curves indicate the Michaelis-Menten behavior of the proposed biosensor [87]. With a sensitivity of approximately 2.5 mA cm^{-2} M^{-1} for flat PPy(DBS) surface, the sensitivity was nearly a quarter of that shown with CNT/PPy(DBS). The unfunctionalized CNT sample did not exhibit a significant reaction, indicating the need to functionalize the material and take advantage of its high surface volume and excellent carrier mobility capabilities. The same experimental procedure with samples not including GA/GOx has been performed and demonstrated in Figure S7.

C. *Selective Glucose Sensing*

Figure 5 shows the addition of common interferents into the buffer for glucose biosensing applications. The PDMS/CNT/PPy(DBS)/GOx was evaluated towards potential interferences commonly present in physiological fluids by studying their response current. AA, urea, NaCl, UA were added into a 1.5 mM glucose solution to reach concentrations of 0.1 mM, 10 mM, 150 mM, and 0.1 mM, respectively, which are common concentrations of these analytes in human physiological fluid samples. Here, the low voltage operation and selective nature of GOx contributed to the use of the sensor towards selective sensing of glucose without significant oxidation of unwanted substances. The long-term durability of a similar stretchable electrode structure of PDMS/VACNT was also tested in our previous work [60], demonstrating its stability and robustness despite repetitive mechanical deformations towards potential wearable applications.

D. *Glucose Sensing with Strain*

The tensile strain was applied to the PDMS/CNT/PPy(DBS)/GOx electrode to demonstrate its use in developing stretchable glucose sensors. In this case, a CNT electrode was fabricated on the same PDMS substrate as a CNT/PPy(DBS)/GOx electrode with a gap between the two electrodes; a drop of a buffer was placed atop of the sensor with subsequent glucose additions for concentration-dependent measurements of glucose. As shown in Figure 6a, the gap between CNT electrodes increased on a millimeter-scale as the tensile strain was applied. The buffer solution was a liquid solution containing glucose and overlapped both electrodes on top as a droplet to simulate physiological fluid. The buffer solution was not a solid or gel, and it did not experience any pertinent mechanical/electromechanical effects from the underlying electrode stretching. Also, the solution resistance is low for phosphate buffer solution, and the distance does not significantly affect its circuit performance [88]. The effect of the gap widening with induced strain between the two electrodes was analogous to placing two electrodes in a beaker of liquid and separating them by several millimeters, which does not significantly affect the diffusion of glucose [89]; if we move two electrodes several millimeters away from each other in an aqueous environment, we will not expect to see an observable change in the electron transfer (given the conductivity of the liquid). Thus, the generated current would also be similar despite the relative change in location by several millimeters. These principles, in theory, apply to both the stretched and unstretched state; ultimately, the electrode distance must maintain continuous contact between both electrodes via the testing solution. If the liquid spans between the two electrodes, it allows the formation of a complete circuit for the application of a constant voltage with current flowing from the electrode, through the conductive solution, and to the opposing electrode.

The current response upon successive addition of 0.8 mM of glucose under tensile strain shown in Figure 6b demonstrated the use of the sensor towards wearable applications. Reliable electrochemical performance under various tensile strains (i.e., stretching up to 75%) was demonstrated with correlation coefficients greater than 0.982, indicating a reliable linear

sensing capability of glucose concentrations with strain up to 75%. As shown in Figure 6c, levels of strains were applied of 0%, 15%, 30%, 45%, 60%, and 75%, corresponding to correlations of determinations of 0.992, 0.987, 0.986, 0.985, 0.990, and 0.982, respectively. Table S3 shows these results and percent differences, demonstrating that all values have less than 1% difference. The sensitivity of this sensor design was approximately 10 mA cm^{-2} M^{-1}, which, as shown by Table S2, is comparable to or exceeds many state-of-the-art flexible glucose sensors. The sensor achieved 90% of steady-state current in less than 3 seconds, enabling the sensor for continuous monitoring [79, 80]. As shown in the literature, general requirements of continuous glucose monitoring in the treatment of diabetes are dictated by the expected fluctuations in glucose levels with a response time of shorter than 5 minutes [90].

Though higher strains are attainable with this electrode design, a strain-dependent performance is observed with strains greater than 75%, as shown in Figure S8. We attribute this to the induced strain resulting in increased resistance as neighboring CNTs make fewer connections. As strain increases, neighboring CNTs spread and may lose some contact (i.e., electronic pathways) with neighboring nanotubes, resulting in a strain-dependent change in resistance. Though this effect is not observable at strains up to 75%, we observe this change in resistance at higher strains.

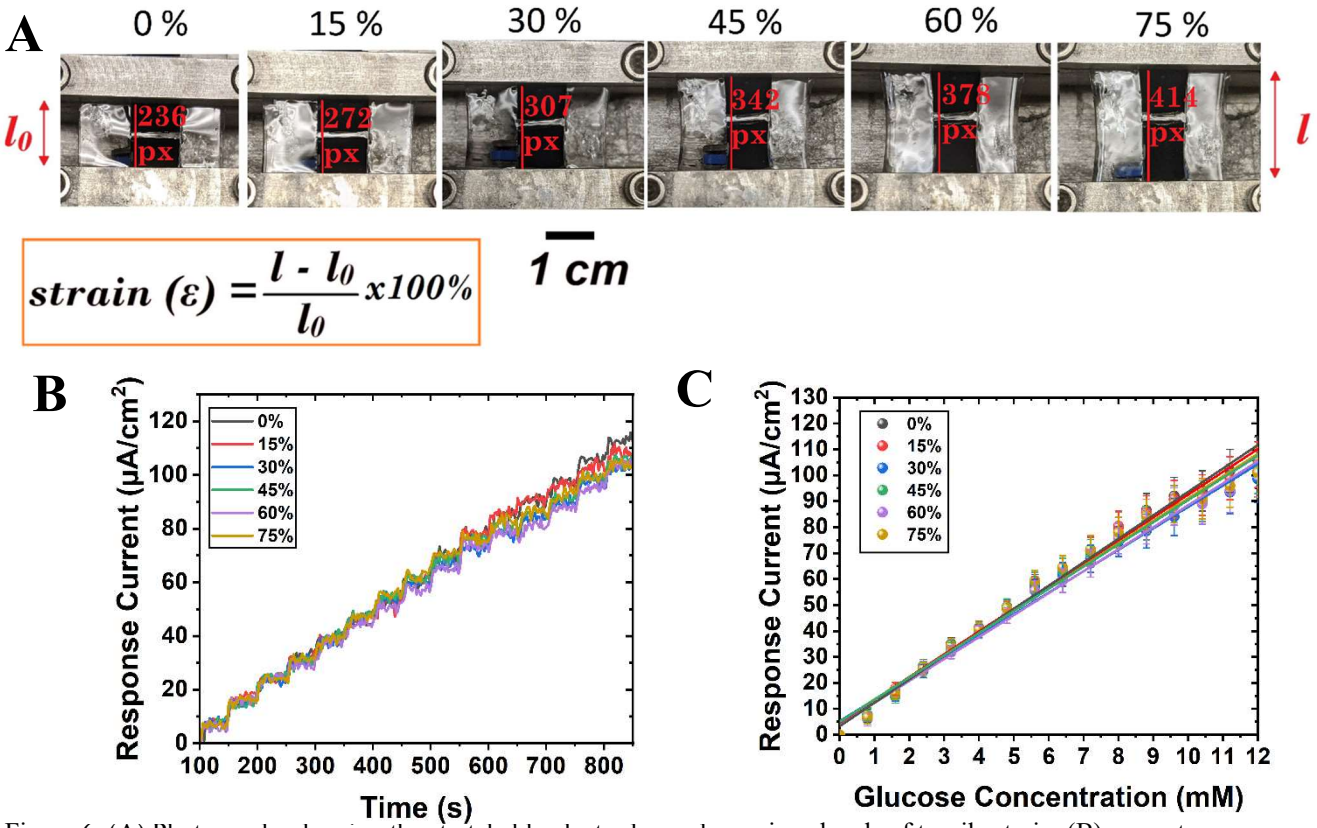

Figure 6. (A) Photographs showing the stretchable electrodes under various levels of tensile strain, (B) current response upon successive addition of 0.8 mM of glucose under strain, and (C) linear calibration curves between the current and the glucose concentration. The lines of the same colors as the data points in the graph correspond to the lines of the linear fit of those data points at that applied strain.

IV. Conclusion

We have demonstrated a stretchable glucose sensor using a PDMS/CNT/PPy(DBS)/GOx electrode. VACNTs were transferred and rooted into the stretchable elastomeric polymer substrate, allowing neighboring CNTs to interconnect for electron transfer with applied tensile strain. The exposed CNTs were conformally coated with a thin film of PPy(DBS), allowing a high surface area and increased reaction sites towards higher sensitivity glucose sensing. The PDMS/CNT/PPy(DBS) sensor achieves 90% of steady-state current in less than 3 seconds, and this response time enables the use of this system for continuous monitoring systems. A sensitivity of approximately 10 mA cm^{-2} M^{-1} and a wide range is observed with glucose concentrations as low as 0.1 mM and up to 12 mM with a highly linear response trend. A strong correlation between the average current response of four different sensors with a coefficient of determination of 0.998, a consistent amount among the different regions of increasing additions of glucose concentration. The sensor was demonstrated towards stretchable sensing applications with an application of tensile strain up to 75% at intervals of 0%, 15%, 30%, 45%, 60%, and 75%; the performance of the sensor under each strain application demonstrated a coefficient of determination greater than 0.982, indicating a reliable linear sensing capability of glucose concentrations. These results show the potential of the stretchable biosensors towards potential wearable applications interfacing with physiological fluids.

V. REFERENCES

[1] Z. Lou et al., "Ultrasensitive and ultraflexible e-skins with dual functionalities for wearable electronics," *Nano Energy*, 38 (March), 28–35, (2017).

[2] H. Derakhshandeh et. al., "Smart bandages: The future of wound care," *Trends in Biotechnology*, 36 (12), 1259–1274, (2018).

[3] L. Lu et. al, "Wearable health devices in health care: Narrative systematic review," *JMIR mHealth and uHealth*, 8 (11), e18907, (2020).

[4] Y. Tang et al., "Highly stretchable and ultrasensitive strain sensor based on reduced graphene oxide microtubes–elastomer composite," *ACS Applied Materials & Interfaces*, 7 (49), 27432–27439, (2015).

[5] S. Huang et al., "Flexible electronics: Stretchable electrodes and their future," *Advanced Functional Materials*, 29 (6), 1805924, (2019).

[6] T. Yamada et al., "A stretchable carbon nanotube strain sensor for human-motion detection," *Nature Nanotechnology*, 6 (5), 296, (2011).

[7] G. Ge et al., "Stretchable, transparent, and self-patterned hydrogel-based pressure sensor for human motions detection," *Advanced Functional Materials*, 28 (32), 1–8, (2018).

[8] Y. Wang et al., "Wearable and highly sensitive graphene strain sensors for human motion monitoring," *Advanced Functional Materials*, 24 (29), 4666–4670, (2014).

[9] M. M. Rodgers et al., "Recent advances in wearable sensors for health monitoring," *IEEE Sensors Journal*, 15 (6), 3119–3126, (2014).

[10] D. Bruen et al., "Glucose sensing for diabetes monitoring: Recent developments," *Sensors (Switzerland)*, 17 (8), 1–22, (2017).

[11] S. C. Mukhopadhyay, "Wearable sensors for human activity monitoring: A review," *IEEE Sensors Journal*, 15 (3), 1321–1330, (2014).

[12] R. He et al., "Flexible Miniaturized Sensor Technologies for Long-Term Physiological Monitoring," npj Flexible Electronics, 6 (1), 20, (2022).

[13] J.-S. Noh, "Conductive elastomers for stretchable electronics, sensors and energy harvesters," *Polymers*, 8 (4), 123, (2016).

[14] C. Yan et al., "Stretchable energy storage and conversion devices," *Small*, 10 (17), 3443–3460, (2014).

[15] H. Kudo et al., "A flexible and wearable glucose sensor based on functional polymers with Soft-MEMS techniques," *Biosensors and Bioelectronics*, 22 (4 SPEC. ISS.), 558–562, (2006).

[16] J. J. Mastrototaro et al., "An electroenzymatic glucose sensor fabricated on a flexible substrate," *Sensors and Actuators B: Chemical*, 5 (1–4), 139–144, (1991).

[17] M. A. Abrar et al., "Bendable electro-chemical lactate sensor printed with silver nano-particles," *Scientific Reports*, 6 (1), 1–9, (2016).

[18] J. R. Fleming et al., "Mechanics of crack propagation in delamination wear," Wear, 44 (1), 39–56, (1977).

[19] T. Cheng et al., "Stretchable thin-film electrodes for flexible electronics with high deformability and stretchability," *Advanced Materials*, 27 (22), 3349–3376, (2015).

[20] W. S. Wong et al., Flexible electronics: Materials and applications, 11. *Springer Science & Business Media*, 2009.

[21] M. B. Jakubinek et al.,"Thermal and electrical conductivity of tall, vertically aligned carbon nanotube arrays," *Carbon*, 48 (13), 3947–3952, (2010).

[22] P. Mishra et al., "Transfer of microstructure pattern of CNTs onto flexible substrate using hot press technique for sensing applications," *Materials Research Bulletin*, 48 (8), 2804–2808, (2013).

[23] B. Zhou et al., "Interfacial adhesion enhanced flexible polycarbonate/carbon nanotubes transparent conductive film for vapor sensing," *Composites Communications*, 15, 80–86, (2019).

[24] S. Kumar et al., "Review—recent advances in the development of carbon nanotubes based flexible sensors," *Journal of The Electrochemical Society*, 167 (4), 047506, (2020).

[25] M. Nankali et al., "Highly stretchable and sensitive strain sensors based on carbon nanotube–elastomer nanocomposites: The effect of environmental factors on strain sensing performance," *Journal of Materials Chemistry C*, 8 (18), 6185–6195, (2020).

[26] X. Luo et al., "Enhancement of a conducting polymer-based biosensor using carbon nanotube-doped polyaniline," *Analytica Chimica Acta*, 575 (1), 39–44, (2006).

[27] G. Tadayyon et al., "In vitro analysis of a physiological strain sensor formulated from a PEDOT: PSS functionalized carbon nanotube-poly (glycerol sebacate urethane) composite," *Materials Science and Engineering: C*, 121, 111857, (2021).

[28] Y. Zhang et al., "Fiber organic electrochemical transistors based on multi-walled carbon nanotube and polypyrrole composites for noninvasive lactate sensing," *Analytical and Bioanalytical Chemistry*, 412 (27), 7515–7524, (2020).

[29] X. Luo et al., "Enhancement of a conducting polymer-based biosensor using carbon nanotube-doped polyaniline," *Analytica Chimica Acta*, 575 (1), 39–44, (2006).

[30] G. Z. Chen et al., "Carbon nanotube and polypyrrole composites: Coating and doping," *Advanced Materials*, 12 (7), 522–526, (2000).

[31] C.-C. Hu et al., "Ideally capacitive behavior and x-ray photoelectron spectroscopy characterization of polypyrrole," *Journal of The Electrochemical Society*, 149 (8), A1049, (2002).

[32] K. Naoi et al., "Electrochemistry of surfactant-doped polypyrrole film(I): Formation of columnar structure by electropolymerization," *Journal of The Electrochemical Society*, 142 (2), 417–422, (1995).

[33] S. B. Adeloju et al., "Fabrication of ultra-thin polypyrrole–glucose oxidase film from supporting electrolyte-free monomer solution for potentiometric biosensing of glucose," *Biosensors and Bioelectronics*, 16 (3), 133–139, (2001).

[34] B. Haghighi et al., "Direct electron transfer from glucose oxidase immobilized on an overoxidized polypyrrole film decorated with Au nanoparticles," *Colloids and Surfaces B: Biointerfaces*, 103, 566–571, (2013).

[35] R. Jain et al., "Polypyrrole based next generation electrochemical sensors and biosensors: A review," *TrAC Trends in Analytical Chemistry*, 97, 363–373, (2017).

[36] Y. Wang et al., "The woven fiber organic electrochemical transistors based on polypyrrole nanowires/reduced graphene oxide composites for glucose sensing," *Biosensors and Bioelectronics*, 95, 138–145, (2017).

[37] M. Abdolrazzaghi et al., "Noninvasive Glucose Sensing in Aqueous Solutions Using an Active Split-Ring Resonator," *IEEE Sensors Journal*, 21 (17), 18742–18755, (2021).

[38] M. Abdolrazzaghi et al., "Techniques to Improve the Performance of Planar Microwave Sensors: A Review and Recent Developments," *Sensors*, 22 (18). 2022.

[39] E. Muslu et al., "Prussian Blue-Based Flexible Thin Film Nanoarchitectonics for Non-enzymatic Electrochemical Glucose Sensor," *Journal of Inorganic and Organometallic Polymers and Materials*, 32 (8), 2843–2852, (2022).

[40] Z. Pu et al., "A flexible electrochemical glucose sensor with composite nanostructured surface of the working electrode," *Sensors and Actuators B: Chemical*, 230, 801–809, (2016).

[41] Y. Zhang et al., "A flexible non-enzymatic glucose sensor based on copper nanoparticles anchored on laser-induced graphene," *Carbon*, 156, 506–513, (2020).

[42] Y. Zhao et al., "Highly stretchable and strain-insensitive fiber-based wearable electrochemical biosensor to monitor glucose in the sweat," *Analytical Chemistry,* 91 (10), 6569–6576, (2019).

[43] A. J. Bandodkar et al., "Highly stretchable fully-printed CNT-based electrochemical sensors and biofuel cells: Combining intrinsic and design-induced stretchability," *Nano letters*, 16 (1), 721–727, (2016).

[44] X. Jin et al., "Fully integrated flexible biosensor for wearable continuous glucose monitoring," *Biosensors and Bioelectronics*, 196, 113760, (2022).

[45] S. Lin et al., "A flexible and highly sensitive nonenzymatic glucose sensor based on DVD-laser scribed graphene substrate," *Biosensors and Bioelectronics*, 110, 89–96, (2018).

[46] S. Y. Oh et al., "Skin-attachable, stretchable electrochemical sweat sensor for glucose and pH detection," *ACS Applied Materials and Interfaces*, 10 (16), 13729–13740, (2018).

[47] P. T. Toi et al., "Highly electrocatalytic, durable, and stretchable nanohybrid fiber for on-body sweat glucose detection," *ACS Applied Materials & Interfaces*, 11 (11), 10707–10717, (2019).

[48] V. Myndrul et al., "MXene nanoflakes decorating ZnO tetrapods for enhanced performance of skin-attachable stretchable enzymatic electrochemical glucose sensor," *Biosensors and Bioelectronics*, 207, 114141, (2022).

[49] C. W. Bae et al., "Fully stretchable capillary microfluidics-integrated nanoporous gold electrochemical sensor for wearable continuous glucose monitoring," *ACS Applied Materials & Interfaces*, 11 (16), 14567–14575, (2019).

[50] H. Yoon et al., "A chemically modified laser-induced porous graphene based flexible and ultrasensitive electrochemical biosensor for sweat glucose detection," *Sensors and Actuators B: Chemical*, 311, 127866, (2020).

[51] A. Abellán-Llobregat et al., "A stretchable and screen-printed electrochemical sensor for glucose determination in human perspiration," *Biosensors and Bioelectronics*, 91, 885–891, (2017).

[52] Y. Shu et al., "Highly stretchable wearable electrochemical sensor based on Ni-Co MOF nanosheet-decorated Ag/rGO/PU fiber for continuous sweat glucose detection," *Analytical Chemistry*, 93 (48), 16222–16230, (2021).

[53] Y. C. Tsai et al., "Electrodeposition of polypyrrole-multiwalled carbon nanotube-glucose oxidase nanobiocomposite film for the detection of glucose," *Biosensors and Bioelectronics*, 22 (4 SPEC. ISS.), 495–500, (2006).

[54] J. Wang et al., "Carbon-nanotubes doped polypyrrole glucose biosensor," *Analytica Chimica Acta*, 539 (1–2), 209–213, (2005).

[55] M. Raicopol et al., "Functionalized single-walled carbon nanotubes/polypyrrole composites for amperometric glucose biosensors," *Nanoscale Research Letters*, 8 (1), 1–8, (2013).

[56] K. Singh et al., "Fabrication of amperometric bienzymatic glucose biosensor based on MWCNT tube and polypyrrole multilayered nanocomposite," *Journal of Applied Polymer Science*, 125 (S1), E-235-E246, (2012).

[57] B. K. Shrestha et al., "High-performance glucose biosensor based on chitosan-glucose oxidase immobilized polypyrrole/Nafion/functionalized multi-walled carbon nanotubes bio-nanohybrid film," *Journal of Colloid and Interface Science*, 482, 39–47, (2016).

[58] B. K. Shrestha et al., "Globular shaped polypyrrole doped well-dispersed functionalized multiwall carbon nanotubes/nafion composite for enzymatic glucose biosensor application*," Scientific Reports*, 7 (1), 1–13, (2017).

[59] V. Brânzoi et al., "Amperometric glucose biosensor based on electropolymerized carbon nanotube/polypyrrole composite film," *Revue Roumaine de Chimie,* 54 (10), 783–789, (2009).

[60] R. Zhang et al., "A flexible pressure sensor with sandwiched carpets of vertically aligned carbon nanotubes partially embedded in polydimethylsiloxane substrates," *IEEE Sensors Journal*, 20 (20), 12146–12153, (2020).

[61] R. Zhang et al., "Highly stretchable supercapacitors enabled by interwoven CNTs partially embedded in PDMS," *ACS Applied Energy Materials*, 1 (5), 2048–2055, (2018).

[62] J. Ding et al., "Graphene—vertically aligned carbon nanotube hybrid on PDMS as stretchable electrodes," *Nanotechnology*, 28 (46), 465302, (2017).

[63] R. Zhang et al., "A stretchable and bendable all-solid-state pseudocapacitor with dodecylbenzenesulfonate-doped polypyrrole-coated vertically aligned carbon nanotubes partially embedded in PDMS," *Nanotechnology*, 30 (9), (2019).

[64] H. Liu et al., "Study on Direct Electrochemistry of Glucose Oxidase Stabilized by Cross-Linking and Immobilized in Silica Nanoparticle Films," *Electroanalysis: An International Journal Devoted to Fundamental and Practical Aspects of Electroanalysis*, 19 (7-8), 884–892, (2007).

[65] V. K. Gade et al., "Immobilization of GOD on electrochemically synthesized Ppy–PVS composite film by cross-linking via glutaraldehyde for determination of glucose," *Reactive and functional polymers*, 66 (12), 1420–1426, (2006).

[66] S. Avrameas et al., "The cross-linking of proteins with glutaraldehyde and its use for the preparation of immunoadsorbents," *Immunochemistry*, 6 (1), 53–66, (1969).

[67] S. Yoon et al., "Cost-effective stretchable Ag nanoparticles electrodes fabrication by screen printing for wearable strain sensors," *Surface and Coatings Technology*, 384, 125308, (2020).

[68] M. Al-Rubaiai et al., "A 3D-printed stretchable strain sensor for wind sensing," *Smart Materials and Structures*, 28 (8), 84001, (2019).

[69] X. Zhou et al., "Fabrication of highly stretchable, washable, wearable, water-repellent strain sensors with multi-stimuli sensing ability," *ACS Applied Materials & Interfaces*, 10 (37), 31655–31663, (2018).

[70] Y. T. Tsai et al., "Tunable wetting mechanism of polypyrrole surfaces and low-voltage droplet manipulation via redox," *Langmuir*, 27 (7), 4249–4256, (2011).

[71] Y.-T. Tsai et al., "Low-voltage manipulation of an aqueous droplet in a microchannel via tunable wetting on PPy(DBS)," *Lab on a Chip*, 13 (2), 302–309, (2012).

[72] W. Xu et al., "Lateral actuation of an organic droplet on conjugated polymer electrodes via imbalanced interfacial tensions," *Soft Matter*, 12 (33), 6902–6909, (2016).

[73] J. Xu et al., "Effects of electropolymerization parameters of PPy (DBS) surfaces on the droplet flattening behaviors during redox," *The Journal of Physical Chemistry B*, 120 (39), 10381–10386, (2016).

[74] W. Xu et al., "On-demand capture and release of organic droplets using surfactant-doped polypyrrole surfaces," *ACS Applied Materials & Interfaces*, 9 (27), 23119–23127, (2017).

[75] J. Xu et al., "A carbon nanotube-embedded conjugated polymer mesh with controlled oil absorption and surface regeneration via in situ wettability switch," *Journal of Colloid and Interface Science*, 532, 790–797, (2018).

[76] W. Xu et al., "In situ control of underwater-pinning of organic droplets on a surfactant-doped conjugated polymer surface," *ACS Applied Materials & Interfaces*, 7 (46), 25608–25617, (2015).

[77] M. Liu et al., "Self-assembled nanozyme complexes with enhanced cascade activity and high stability for colorimetric detection of glucose," *Chinese Chemical Letters*, 30 (5), 1009–1012, (2019).

[78] M. Moses Phiri et al., "Facile immobilization of glucose oxidase onto gold nanostars with enhanced binding affinity and optimal function," *Royal Society Open Science*, 6 (5), 190205, (2019).

[79] X. Xuan et al., "A wearable electrochemical glucose sensor based on simple and low-cost fabrication supported micro-patterned reduced graphene oxide nanocomposite electrode on flexible substrate," *Biosensors and Bioelectronic*s, 109, 75–82, (2018).

[80] X. Xue et al., "Self-powered electronic-skin for detecting glucose level in body fluid basing on piezo-enzymatic-reaction coupling process," *Nano Energy*, 26, 148–156, (2016).

[81] M. Zeynep Çetin et al., "Utilization of polypyrrole nanofibers in glucose detection," *Journal of the Electrochemical Society*, 164 (12), B585–B590, (2017).

[82] C. Debiemme-Chouvy et al., "Advantage of ultra thin overoxidized polypyrrole membrane in the design of amperometric biosensor," *ECS Transactions*, 33 (8), 21–24, (2010).

[83] P. A. Fiorito et al., "Glucose amperometric biosensor based on the co-immobilization of glucose oxidase (GOx) and ferrocene in poly(pyrrole) generated from ethanol/water mixtures," *Journal of the Brazilian Chemical Society*, 12 (6), 729–733, (2001).

[84] F. R. Duke et al., "Glucose oxidase mechanism. Enzyme activation by substrate," *Journal of the American Chemical Society*, 91 (14), 3904–3909, (1969).

[85] S. B. Bankar et al., "Glucose oxidase - An overview," *Biotechnology Advances*, 27 (4), 489–501, (2009).

[86] M. B. Jakubinek et al., "Thermal and electrical conductivity of tall, vertically aligned carbon nanotube arrays," *Carbon*, 48 (13), 3947–3952, (2010).

[87] L. Michaelis et al., "Die kinetik der invertinwirkung," *Biochemische Zeitschrift*, 49 (333–369), 352, (1913).

[88] S. Gupta et al., "On-chip latex agglutination immunoassay readout by electrochemical impedance spectroscopy," *Lab on a Chip*, 12 (21), 4279–4286, (2012).

[89] S. Ernst et al., "The electrooxidation of glucose in phosphate buffer solutions: Part I. Reactivity and kinetics below 350 mV/RHE," *Journal of Electroanalytical Chemistry and Interfacial Electrochemistry*, 100 (1–2), 173–183, (1979).

[90] G. Reach et al., "Can continuous glucose monitoring be used for the treatment of diabetes," *Analytical Chemistry*, 64 (6), 381A-386A, (1992).